Hierarchical Growth of Chiral Self-Assembled Structures in Protic Media†

L. Brunsveld,‡ H. Zhang,§ M. Glasbeek,§ J. A. J. M. Vekemans,‡ and E. W. Meijer*,‡

Contribution from the Laboratory of Macromolecular and Organic Chemistry, Dutch Polymer Institute, Eindhoven University of Technology, P.O. Box 513, 5600 MB Eindhoven, The Netherlands, and the Laboratory for Physical Chemistry, University of Amsterdam, Nieuwe Achtergracht 129, 1018 WS Amsterdam, The Netherlands

Received February 11, 2000

Abstract: The location of nine chiral penta(ethylene oxide) side chains at the periphery of a C_3-symmetrical hydrogen-bonded extended core gives rise to a thermotropic discotic liquid crystalline material that shows lyotropic phases in polar, protic media. The molecular stacks self-assemble in a reversible and hierarchical fashion, and specific and subtle solvent−molecule interactions together with the created hydrophobic microenvironment account for an unprecedented stabilization of a preferred handedness of the helical stacks by cooperative intermolecular interactions. The presence of either chirality or achirality at the supramolecular level in the stacks can be tuned by temperature and solvent as judged from circular dichroism spectroscopy. A hierarchical growth of the self-assembly is revealed using a variety of spectroscopic techniques and differential scanning calorimetry.

Introduction

Remarkable control of chirality in supramolecular architectures is demonstrated using cooperative hydrogen bonding,[1] often in combination with $\pi-\pi$ stacking.[2,3] It has been shown frequently that chirality present in the solubilizing side chain of a (macro)molecule can be brought to expression at the next hierarchical level of organization by inducing a preference for one of two "supramolecular" conformations.[3−5] Most of these studies to transfer chiral information through molecular assembly are carried out in aprotic organic media, due to the difficulty of using the ensemble of secondary interactions in protic media. As a result, the level of control in well-defined architectures of synthetic chiral structures in protic media by a cooperative action is very limited.[6] This limitation is primarily due to the lack of directionality of hydrophobic interactions and/or the lack of stability of the more directional bonding patterns, such as hydrogen bonding, in protic media. For natural proteins[7] and (synthetic) foldamers,[8] it is known that the stabilization of their supramolecular structure (i.e., their native fold) in polar solvents involves a variety of forces. Hydrophobicity has generally been considered to be the main driving force for the collapse of the random coil, whereas the well-defined 3-D structure is accounted for by interactions such as hydrogen bonding. This specific hydrogen bonding only arises in the created hydrophobic domain of the protein, whereas in the random coil water is interfering. Therefore, synthetic compounds large enough to create hydrophobic microdomains, capable of shielding the more sensitive polar interactions from the protic solvent, should allow the expression of all secondary interactions in a cooperative way and the study of their individual contributions to the formation of chiral superstructures. With this type of synthetic structures, it should be feasible to bridge the gap between manmade "simple" architectures and biomacromolecules and to create new functional systems. Moreover, their properties will serve to aid in the understanding of the distinct differences between superstructure formation in apolar and polar media.

For assemblies in protic solvents, such as chromonics in water, detailed information concerning the conformational uniqueness of the self-assembled state is scarce.[9] Recently it was shown that α,ω-disubstituted sexithiophenes possess one unique chiral self-assembly in protic media that dissociates without an intermediate disordered state of aggregation,[10] similar

* To whom correspondence should be addressed.

† This material is based upon work supported by the NRC Catalysis.

‡ Eindhoven University of Technology.

§ University of Amsterdam.

(1) (a) Rivera, J. M.; Martin, T.; Rebek, J., Jr. *Science* **1998**, *279*, 1021. (b) Simanek, E. E.; Qiao, S.; Choi, I. S.; Whitesides, G. M. *J. Org. Chem.* **1997**, *62*, 2619.

(2) (a) Prins, L. J.; Huskens, J.; de Jong, F.; Timmerman, P.; Reinhoudt, D. N. *Nature* **1999**, *398*, 498. (b) Russell, K. C.; Lehn, J.-M.; Kyritsakas, N.; DeCian, A.; Fischer, J. *New J. Chem.* **1998**, 123.

(3) Palmans, A. R. A.; Vekemans, J. A. J. M.; Havinga, E. E.; Meijer, E. W. *Angew. Chem., Int. Ed. Engl.* **1997**, *36*, 2648.

(4) (a) Yashima, E.; Maeda, K.; Okamoto, Y. Nature **1999**, *399*, 449. (b) Langeveld-Voss, B. M. W.; Waterval, R. J. M.; Janssen, R. A. J.; Meijer, E. W. *Macromolecules* **1999**, *32*, 227. (c) Mayer, S.; Maxein, G.; Zentel, R. *Macromolecules* **1998**, *31*, 8522. (d) Gu, H.; Nakamura, Y.; Sato, T.; Teramoto, A.; Green, M. M.; Jha, S. K.; Andreola, C.; Reidy, M. P. *Macromolecules* **1998**, *31*, 6362. (e) Schlitzer, D. S.; Novak, B. M. *J. Am. Chem. Soc.* **1998**, *120*, 2196. (f) Yashima, E.; Matsushima, T.; Okamoto, Y. *J. Am. Chem. Soc.* **1997**, *119*, 6345. (g) Gulik-Krzywicki, T.; Fouquey, C.; Lehn, J.-M. *Proc. Natl. Acad. Sci. U.S.A.* **1993**, *90*, 163. (h) Green M. M.; Peterson, N. C.; Sato, T.; Teramoto, A.; Cook, R.; Lifson, S. *Science* **1995**, *268*, 1860. (i) Moore, J. S.; Gorman, C. B.; Grubbs, R. H. *J. Am. Chem. Soc.* **1991**, *113*, 1704.

(5) Prince, R. B.; Brunsveld, L.; Meijer, E. W.; Moore, J. S. *Angew. Chem., Int. Ed.* **2000**, *39*, 228.

(6) Bonazzi, S.; DeMorais, M. M.; Gottarelli, G.; Mariani, P.; Spada, G. P. *Angew. Chem., Int. Ed. Engl.* **1993**, *32*, 248.

(7) (a) Creighton, T. E. *Proteins, structures and molecular properties*; W.H. Freeman and Company: New York, 1984. (b) *Prediction of protein structure and the principles of protein conformation*; Fasman, G. D., Ed.; Plenum Press: New York, 1990.

(8) Gellman, S. H. *Acc. Chem. Res.* **1998**, *31*, 173.

(9) For a recent review on chromonics, see: Lydon, J. *Curr. Opin. Colloid Interface Sci.* **1998**, *3*, 458.

(10) Kilbinger, A. F. M.; Schenning, A. P. H. J.; Goldoni, F.; Feast, W. J.; Meijer, E. W. *J. Am. Chem. Soc.* **2000**, *122*, 1820.

10.1021/ja0005237 CCC: $19.00
Published on Web 06/17/2000

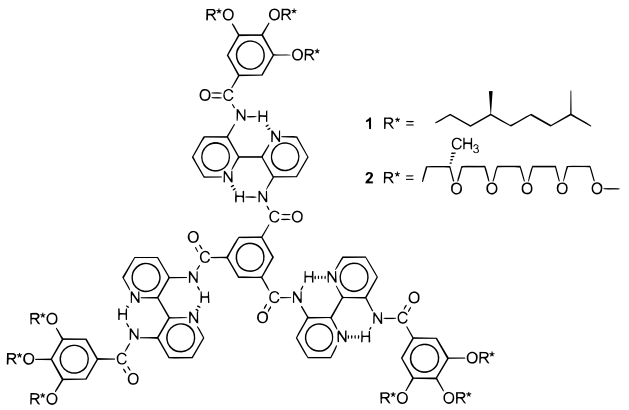

Figure 1. Chiral C_3-symmetrical discotics **1** (apolar) and **2** (polar).

to the behavior of chromonics.[9] Moore et al., however, showed recently that in the folding process of a series of oligo(*m*-phenylene ethynylene)s, first a disordered state is formed before a unique helical conformation is obtained.[5] The hierarchical folding is due to a stepwise occurrence of the diverse interactions; first a hydrophobic collapse of the backbone takes place followed by a structuring process in which the backbone becomes highly ordered together with the side chains.

We have previously shown that hydrogen bonding in the C_3-symmetrical disk-shaped molecule **1** (Figure 1) favors planarity and helps to create chiral columnar aggregates in dilute alkane solutions in a highly cooperative fashion.[3] The homochiral side chains give preference to one helicity in the stacks of these columns for which a cooperativity length of 280 Å (80 molecules) has been determined using a "sergeant-and-soldiers" experiment.[11] The expression of supramolecular chirality is due to positional locking of the molecules that accompanies the self-assembly; such a process is generally observed for supramolecular architectures in apolar media. Here, we demonstrate that chiral columnar aggregates can be formed in polar, protic media when chiral penta(ethylene oxide) side chains are present at the periphery of the hydrogen-bonded extended core. In addition, we show a remarkable and pronounced stepwise growth of the self-assembly in protic solvents. This is in sharp contrast to the self-assembly in apolar solvents. Thus, C_3-symmetrical disk **2** is designed to ensure solubility in polar solvents in order to elucidate the individual contributions of the secondary interactions (Figure 1). By locating the stereochemical information in the side chain as close as possible to the core of the disk, the most favorable cooperative interactions of the side chains were guaranteed.

Results and Discussion

Synthesis and Characterization. The synthesis of chiral (2*S*)-2-methyl-3,6,9,12,15-pentaoxahexadecanol is based on standard synthetic transformations,[12] and the chiral center was derived from ethyl L-lactate (Scheme 1). All products were characterized by ^{1}H and ^{13}C NMR spectroscopy and GC-MS; all compounds had a purity >98%. The synthesis of **2** is based on the consecutive acylation of the two amino groups of 2,2′-bipyridine-3,3′-diamine (**5**).[13] Equimolar reaction of **5** with mesogenic molecule **7** at 0 °C affords monoacylated bipyridine **4** with a remarkable selectivity of 98%. Subsequent 3-fold

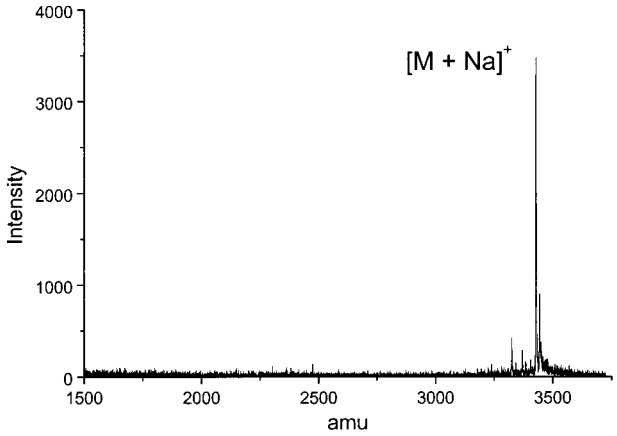

Figure 2. MALDI-TOF mass spectrum of **2**, showing its sodium adduct at $m/z = 3428.1$ (theoretical $m/z = 3428.7$).

Scheme 1. Synthesis of Chiral (2*S*)-2-Methyl-3,6,9,12,15-pentaoxahexadecanol **16**

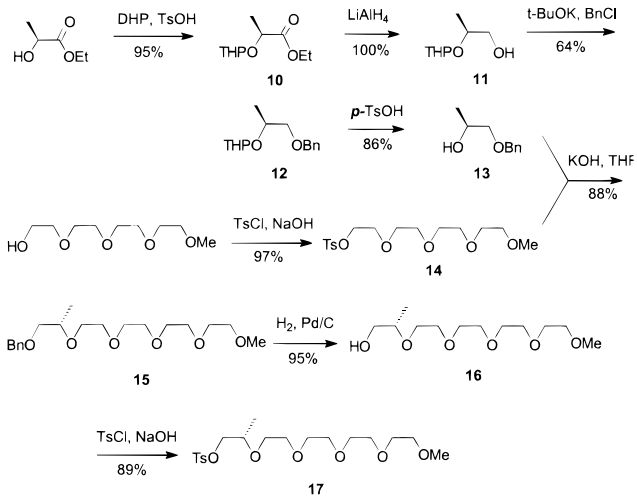

reaction of **4** with trimesic chloride (**3**) gives target compound **2** in an overall yield of 65% from **7** (Scheme 2). Extensive molecular characterization of all molecules is in full agreement with the structures assigned. The characteristic hydrogen-bonded protons in **2** are observed at $\delta = 15.5$ and $\delta = 14.4$ ppm in $CDCl_3$, indicative of the strong hydrogen bonding within the bipyridine unit. As an illustration, the mass spectrum of **2** is depicted in Figure 2.

The thermotropic behavior of **2** was studied using differential scanning calorimetry (DSC) and optical microscopy. The thermotropic mesophase of **2** extends over a broad temperature window; the T_g of **2** was found at −74 °C and the T_{cl} at 270 °C. Typical flowerlike patterns, indicative of a columnar mesophase, are observed under the polarization microscope after slow cooling from the melt.[14]

The aggregation of **2** was studied in various solvents, and we show here the results obtained with a variety of techniques for *n*-butanol in detail (although the results may be generalized

(11) Green, M. M.; Reidy, M. P.; Johnson, R. D.; Darling, G.; O'leary, D. J.; Wilson, G. *J. Am. Chem. Soc.* **1989**, *111*, 6452.

(12) Janssen, H. M.; Peeters, E.; van Zundert, M. F.; van Genderen, M. H. P.; Meijer, E. W. *Macromolecules* **1997**, *9*, 22815.

(13) Palmans, A. R. A.; Vekemans, J. A. J. M.; Fischer, H.; Hikmet, R. A.; Meijer, E. W. *Chem. Eur. J.* **1997**, *3*, 300.

(14) Preliminary X-ray diffraction studies on a series of compounds such as **1** and **2** substituted with different ethylene glycol side chains have elucidated the columnar hexagonal ordered (Col_{ho}) mesophase of these compounds in the liquid crystalline state. Apart from the reflections typical for a Col_{ho} mesophase (100; 110; 200; 210; 001), sharp quadruplet splitted reflections are found in shear aligned samples, suggesting a slight distortion of, or higher order within, the Col_{ho} mesophase, probably due to a regular, helical packing of the molecules within the stacks. For an example, see: Brunsveld, L.; Vekemans, J. A. J. M.; Janssen, H. M.; Meijer, E. W. *Mol. Cryst. Liq. Cryst.* **1999**, *331*, 449 and ref 13.

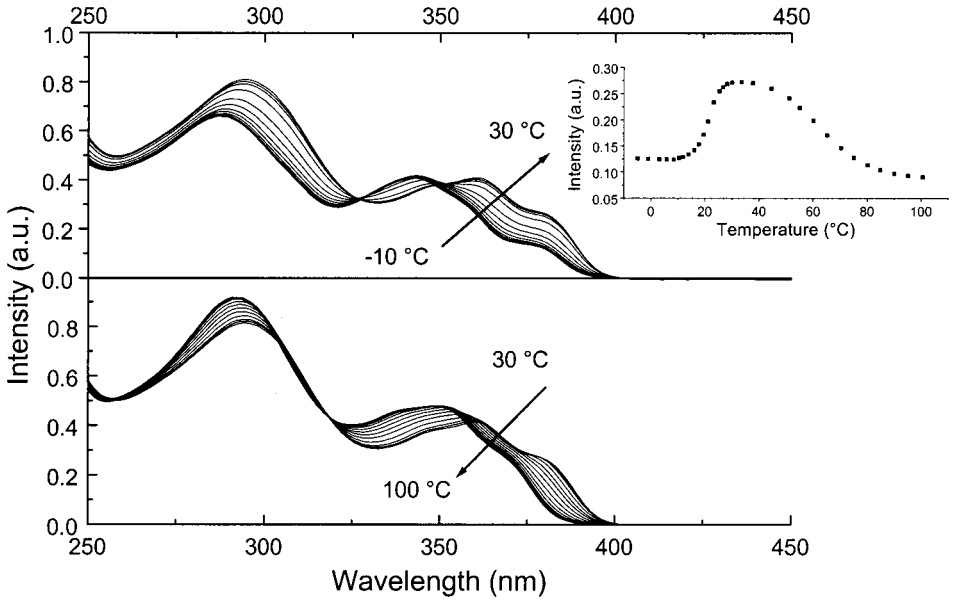

Figure 3. Temperature-dependent UV−vis spectra of **2** in *n*-butanol (2.7×10^{-5} M), showing the two transitions. Top: the increase of the temperature from −10 to 30 °C. Bottom: increase of the temperature from 30 to 100 °C. Inset: the absorbance at 385 nm at different temperatures.

Scheme 2. Synthesis of Disk-Shaped Molecule **2**

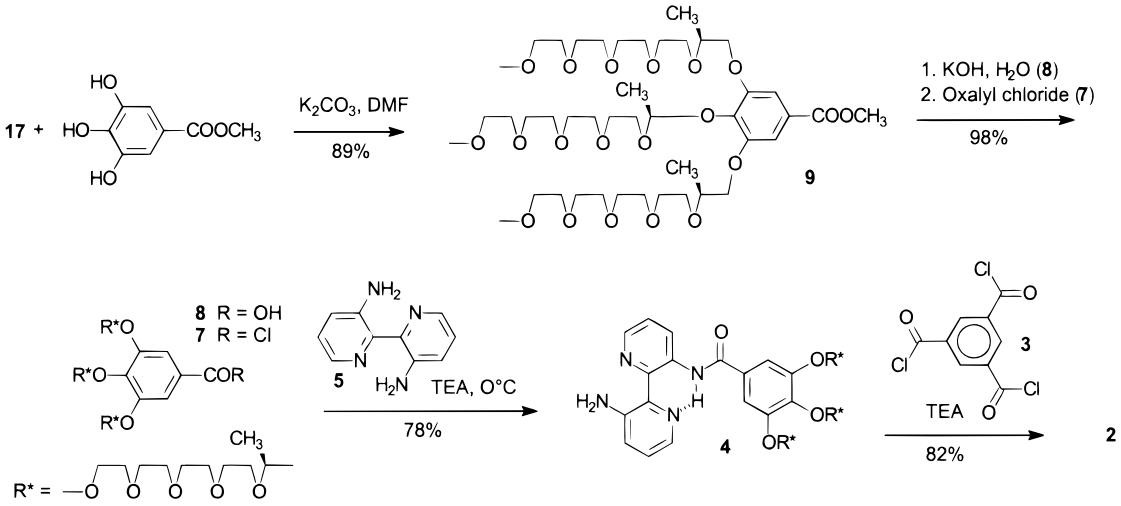

for all low molecular weight alcohols). The higher boiling point of *n*-butanol enables the use of temperature as a tool for denaturation of the self-assembled structures.

UV−Vis and NMR Spectroscopy. Temperature-dependent ultraviolet−visible (UV−vis) absorption (Figure 3) and NMR spectroscopy (Figure 4) measurements were performed in order to investigate the self-assembling of **2** in dilute solution. In chloroform, **2** is molecularly dissolved, as concluded from the shape of the UV spectrum.[3] In polar solvents such as acetonitrile, methanol, ethanol, and *n*-butanol, these molecules aggregate as indicated by the red shift of about 10 nm in the UV spectrum. Raising the temperature of a solution of **2** (10^{-5} M) in *n*-butanol from −10 to 100 °C resulted in two transitions as concluded from the UV spectra (Figure 3). Whereas between −10 and 15 °C the UV spectrum is constant, a highly cooperative transition takes place around 20 °C, resulting in a spectrum that is red-shifted. Further heating gives, above 30 °C, rise to the second transition as evidenced by a gradual blue shift of the spectra. At 100 °C a UV spectrum was obtained which featured the same band shape as that of **2** in chloroform at room temperature. ^{1}H NMR and ^{13}C NMR spectra of compound **2** in deuterated chloroform at room temperature showed clearly resolved spectra indicating the molecularly dissolved nature of **2**. A similarly resolved spectrum was obtained for a 1.5 wt % solution of **2** in *n*-butanol-d_{10} at 100 °C. However, cooling of the *n*-butanol-d_{10} solution to 35 °C gave rise to a gradual broadening of the signals with a concomitant significant shielding of the aromatic protons (Figure 4). Both processes are indicative of aggregation via $\pi-\pi$ stacking and reveal the order within the stacks. Lowering the temperature from 35 to 30 °C resulted in a sudden and complete loss of the signals attributed to the aromatic protons. Lowering the temperature even further did not change the spectrum anymore. This phenomenon is due to the total loss of freedom of movement within the self-assembly. This process is highly cooperative as can be deduced from the sharp S-curve observed with the temperature-dependent UV−vis spectroscopy and the sudden sharp transition observed by ^{1}H NMR spectroscopy.

Time-Resolved Fluorescence Spectroscopy. Time-resolved fluorescence experiments were performed to study the nature of the species in the molecularly dissolved state as well as in the self-assembled structures. To characterize the fluorescence, a comparative study of disk-shaped molecule **2** with model compounds **18a−c** (diacylated 2,2′-bipyridine-3,3′-diamines) was performed (Scheme 3). Analogous to disk-shaped molecule

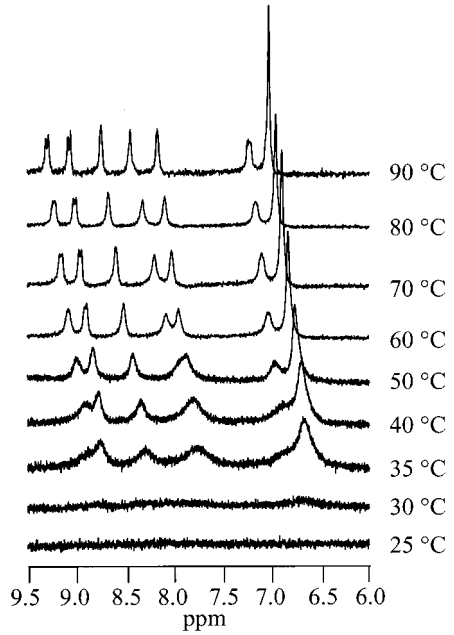

Figure 4. Aromatic region of the ^{1}H NMR spectrum (*n*-butanol-d_{10}, 5×10^{-3} M, 400 MHz) at different temperatures.

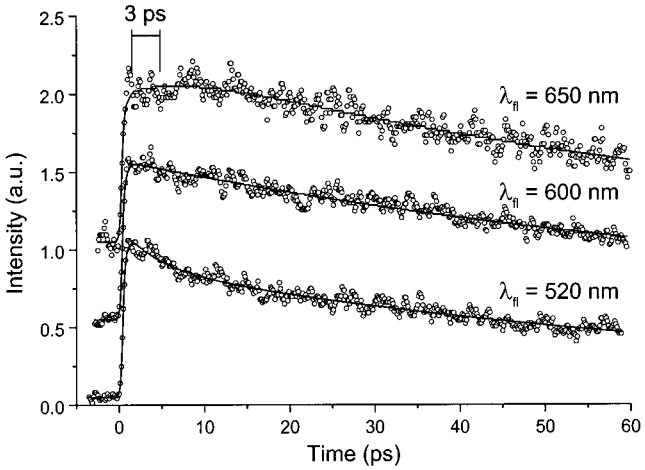

Figure 5. Fluorescence transients of **18c** dissolved in chloroform at room temperature at different detection wavelengths (open circles) with their fits (lines); concentration = 10^{-5} M.

Scheme 3. Model Compounds **18a**−**c**

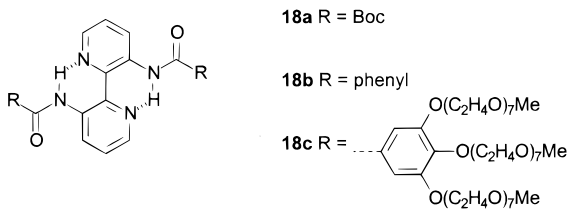

2, all the model compounds showed a large Stokes shift of the fluorescence emission ($\lambda_{max-fluor}$ ~513 nm) under all experimental conditions. Measurements with our femtosecond fluorescence upconversion technique[15] with the detection of emission at different wavelengths, for **18c** in the molecularly dissolved state (in chloroform), showed a dynamic Stokes shift typical of the intramolecular charge transfer; the characteristic time was approximately 3 ps (Figure 5). In analogy with the previously studied 2,2′-bipyridyl-3,3′-diol,[16] it is likely that its fluorescent state refers to a protonated form (obtained after intramolecular proton transfer from the amide to the nitrogen of the heterocycle upon excitation). The dynamic Stokes shift, in typically 3 ps, is representative of the solvation of the photoexcited protonated molecule dissolved in chloroform.[17]

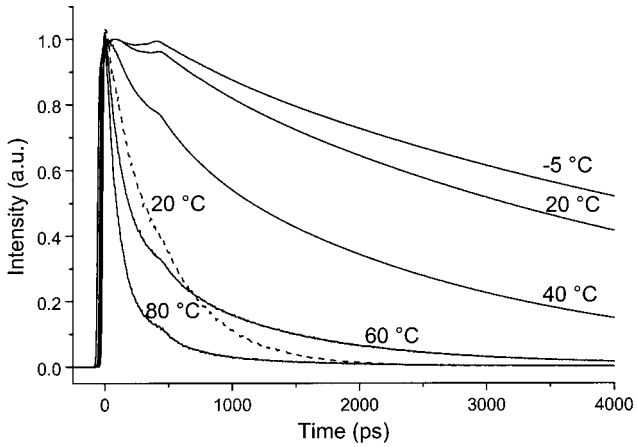

Figure 6. Fitted fluorescence transients of **2** in chloroform (- - -) and in *n*-butanol at different temperatures (—); λ_{fl} = 520 nm; concentration 10^{-6} M. The increase of the transients after ~600 ps is due to the system response and is taken into account with the fitting.

Lifetime measurements were performed using the picosecond fluorescence setup described previously.[18] The excited-state lifetime of the molecularly dissolved compounds in chloroform was found to be dependent on the size of the substituents on the amides. The lifetime of the excited state of compound **18a** is 10 ps; replacement of the Boc group by a phenyl (**18b**) results in an increase of the lifetime to 50 ps. A further enlargement of the steric bulk by attachment of long ethylene oxide chains (**18c**) increases the lifetime to 150 ps.[19] The results thus show that when rigidity is imposed on to the molecules, the nonradiative decay of the excited state is suppressed.

In analogy with these results for compounds **18a**−**c**, it was found that the lifetime of compound **2** had increased from 300 ps in chloroform (molecularly dissolved) to ~5 ns in the self-assembled state, i.e., an increase by about 1 order of magnitude, due to the decreased motion of the molecules within the aggregate. Some typical fluorescence transients fitted to a biexponential function at various temperatures of **2** in chloroform and *n*-butanol (10^{-6} M) are displayed in Figure 6. One of the two characteristic time constants has a magnitude similar to the lifetime for **2** in the molecularly dissolved molecules in chloroform, whereas the second lifetime component is about 1 order of magnitude longer. This finding shows the simultaneous presence of two forms of **2** in solution, i.e., **2** in its molecularly dissolved form and in an aggregated form. It proved impossible to detect the dynamic Stokes shift in the aggregates of **2** in an accurate way. As a result, the time-resolved fluorescence data are focused on the equilibrium between the molecularly dissolved and aggregated forms only (the transition lies between 30 and 90 °C as was already established from UV−vis and NMR spectroscopy, vide supra).

(15) van der Meulen, P.; Zhang, H.; Jonkman, A. M.; Glasbeek, M. *J. Phys. Chem.* **1996**, *100*, 5367.

(16) (a) Prosposito, P.; Marks, D.; Zhang, H.; Glasbeek, M. *J. Phys. Chem. A* **1998**, *102*, 8894. (b) Eyal, M.; Reisfeld, R.; Chernyak, V.; Kaczmarek, L.; Grabowska, A. *Chem. Phys. Lett.* **1991**, *176*, 531. (c) Bulska, H. *Chem. Phys. Lett.* **1983**, *98*, 398.

(17) Horng, M. L.; Gardecki, J. A.; Papazyan, A.; Maroncelli, M. *J. Phys. Chem.* **1995**, *99*, 17311.

(18) Middelhoek, E. R.; van der Meulen, P.; Verhoeven, J. W.; Glasbeek, M. *Chem. Phys.* **1995**, *198*, 373.

(19) Transients were found to be independent of the detection wavelength (520, 570, and 620 nm).

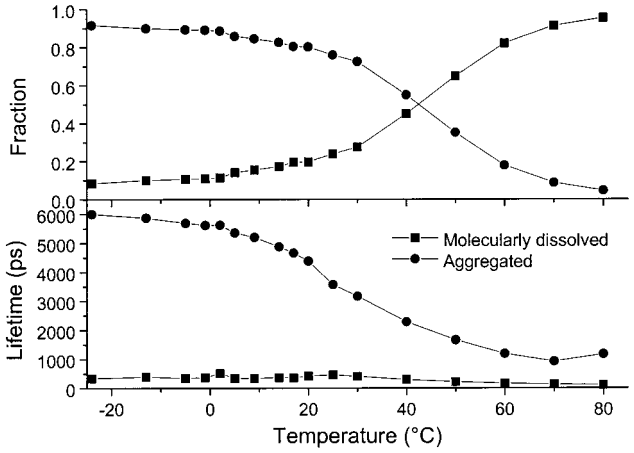

Figure 7. Top: fraction of aggregated molecules (circles) and molecularly dissolved molecules (squares) in a 10^{-6} M *n*-butanol solution at different temperatures. Bottom: lifetimes of the two species, aggregated (circles) and single molecules (squares), as a function of temperature in the same solution.

Figure 7 displays the ratios of compounds being molecularly dissolved and self-assembled at different temperatures. The data reveal that at 80 °C all molecules **2** are molecularly dissolved. Lowering the temperature to 20 °C results in the formation of small aggregates and below 20 °C almost all molecules participate in aggregates. The lifetime of the aggregated species increases rapidly upon lowering the temperature to 20 °C (Figure 7). The increase of the lifetime is due to the formation of aggregates in which the flexibility of the molecules is decreased.

Circular Dichroism and Differential Scanning Calorimetry Studies. Circular dichroism (CD) spectroscopy measurements were performed in order to investigate the expression of chirality and thus the order in the self-assemblies of **2** in dilute solution. Since **2** is molecularly dissolved in chloroform solutions, no well-defined order exists and the side chains cannot interact cooperatively to transfer their chirality to the aromatic core; hence, no detectable CD effect is observed. In polar solvents, however, these molecules do aggregate, which allows intermolecular side-chain interactions to occur. Surprisingly, a significant Cotton effect in the $\pi-\pi^*$ transition is observed at temperatures below 20−30 °C. Apparently the molecules have a high degree of order within the self-assembly which, together with the ordered side chains, results in the formation of a chiral superstructure. To investigate the degree of order during self-assembly, we studied the CD effect for a solution of **2** in *n*-butanol as a function of temperature (Figure 8). Raising the temperature from −10 to 90 °C in steps of 2 °C with ample time to equilibrate resulted in a highly cooperative transition at 20 °C, i.e., the same temperature as the low-temperature transition observed with UV−vis and ^{1}H NMR spectroscopy. At temperatures below the transition, the chirality within the self-assembly is constant, but during the transition the self-assembly totally loses its supramolecular chirality, as concluded from the rapid disappearance of the Cotton effect at 20 °C. These results show that in the self-assembly at low temperatures the molecules are locked in position and nearly all molecules participate in the self-assembly. Consequently, the side chains interact in a cooperative fashion and transfer their chirality to the aromatic core of the disks. At temperatures above this transition, the molecules have lost their positional order, because the intermolecular interactions accounting for that are not operative. The temperature window over which the chirality is lost is only slightly concentration dependent (Figure 9); over a concentration range from 10^{-6} to 10^{-2} M the transition temperature only changes by 10 °C (around 20 °C at 10^{-6} M to 30 °C at 10^{-2} M), in agreement with the transitions observed with UV−vis and ^{1}H NMR spectroscopy. The cooperativity of the transition increases significantly at higher concentrations as deducible from the increase of the sharpness of the transition (Figure 9).

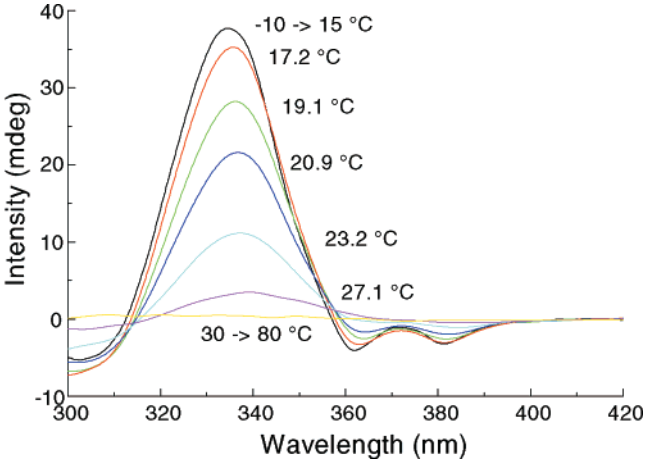

Figure 8. Temperature-dependent CD spectra of **2** in *n*-butanol (10^{-5} M).

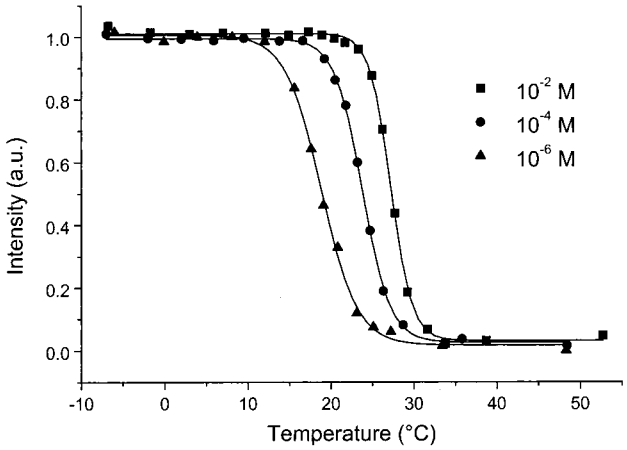

Figure 9. Normalized intensities of the CD spectra of **2** in *n*-butanol at 337 nm at three different concentrations (10^{-6}, 10^{-4}, and 10^{-2} M).

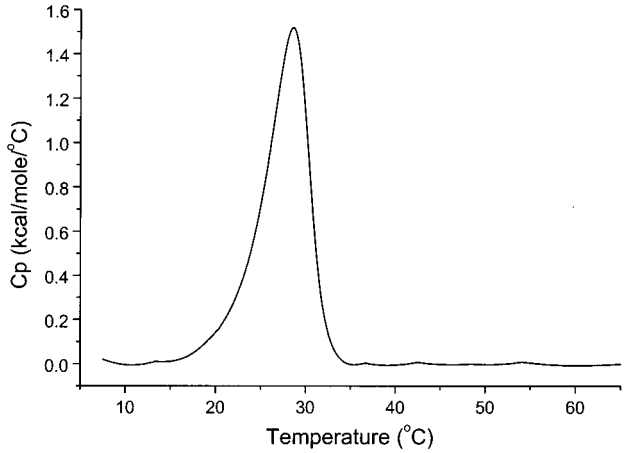

Figure 10. DSC thermodiagram of 3×10^{-5} M of **2** in *n*-butanol.

The transition around 25 °C could also be detected using an ultrasensitive differential scanning calorimeter (DSC) (Figure 10). At 10^{-2} M in *n*-butanol, a melting endotherm could be detected with the melting point at 30 °C and a melting enthalpy of approximately 50 kJ/mol. The transition shifts to lower

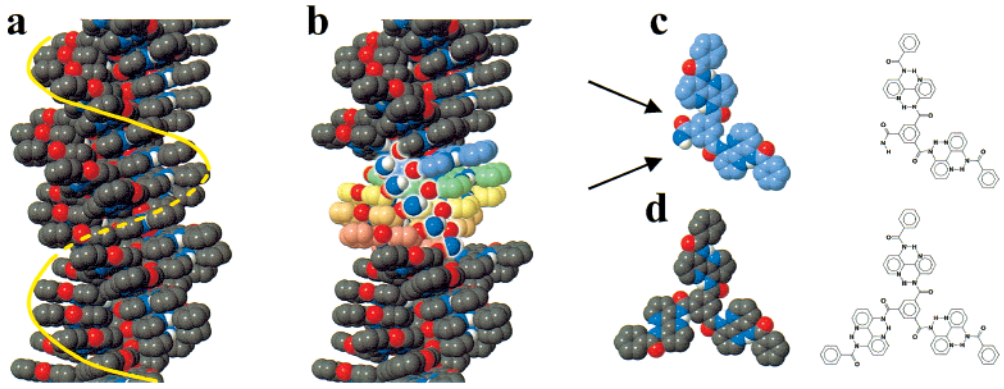

Figure 11. A tentative picture displaying the molecules packed in a chiral column with a pitch of nine molecules (**a**); the chiral side chains have been omitted for clarity. Structure **b** shows the same column, but for the colored molecules one of the outer benzene rings and one of the bipyridine groups have been left out, enabling a look into the core of the column. Highlighted are the intermolecular hydrogen bonds that are proposed to lock the molecules in the column. Structure **c** shows one of the molecules in which parts have been omitted; the arrows indicate the C═O and N−H involved in hydrogen bonding. Structure **d** is the aromatic core of **2** without chiral side chains. The three bipyridine wedges are tilted, similar to the situation in columns **a** and **b**.

temperatures upon lowering the concentration (26.5 °C at 5×10^{-4} M); the energy of the transition remains constant over the concentration range in which measurements could be performed (10^{-2} to 10^{-4} M). These results show the high cooperativity of the transition, while the large energy involved reveals that very strong and specific interactions between the molecules are present. The large energy of the transition also shows that a highly significant growth of the aggregates occurs during the transition, concomitant with the occurrence of the directional intermolecular interactions.

The UV−vis and CD signal near the transition midpoint around 20 °C can be modeled as a linear combination of the signals from the two limiting states (at 10 and 30 °C). Furthermore, the UV−vis and CD data show coinciding sigmoidal transition curves. These results together with the observation of a melting endotherm indicate that the transition from chiral to achiral self-assembly has a two-state behavior.[20] The two limiting states are both present and interconvert. The second transition at higher temperature seems to be less cooperative and follows isodesmic behavior.[9]

The Hierarchical Growth. The dynamic behavior of **2** in *n*-butanol with two different kinds of self-assemblies sharply contrasts with that of apolar analogue **1** in hexane and supramolecular architectures in apolar solvents in general. Upon heating the hexane solution of **1**, optical activity and stacking are lost simultaneously over a broad temperature range (0−100 °C). Hence, aggregation and expression of chirality of the self-assembled stacks of **1** are strongly interrelated. This is due to the apolar solvent, which does not differentiate between ordering secondary interactions (like hydrogen bonding) and the other interactions (like $\pi-\pi$ stacking and hydrophobic interactions) that account for the aggregation. In polar solvents, however, the solvent is capable of preferentially interfering with certain secondary interactions. Owing to its polar nature, *n*-butanol is capable of destroying the structuring secondary interactions between the molecules that account for the positional order in the chiral supramolecular self-assembly. At the low temperatures where this interference starts to take place (∼20 °C), the solubilizing power of *n*-butanol is not sufficient to overcome the hydrophobic $\pi-\pi$ interactions between the aromatic cores. Therefore, the expression of chirality is lost prior to the loss of aggregation and two unique self-assembled states exist, one that expresses its chirality in the supramolecular assembly and one that does not. On the basis of the results presented here, it is proposed that the former is a rigid-rod extended stack, while the disordered aggregate is of small dimensions. Theoretical studies and detailed small-angle neutron scattering (SANS) measurements will be performed to elucidate this in a comprehensive way; notwithstanding, a tentative picture displaying the unique chiral columnar self-assembly is displayed in Figure 11. Preliminary SANS measurements confirm the results above and show the presence of rigid columnar architectures at temperatures below 20 °C.

The hierarchical growth of the self-assembly of **2** contrasts with the behavior of the α,ω-disubstituted sexithiophenes, which only show one unique self-assembly that is proposed to melt upon increasing the temperature.[10] This different behavior is due to the additional intermolecular interactions between molecules of **2** not present in the α,ω-disubstituted sexithiophene. The aggregation of the latter is basically the result of only hydrophobic interactions, whereas **2** has the possibility for extra, solvent dependent, interactions. A two-step process, however, was observed for a series of oligo(*m*-phenylene ethynylene)s.[5] Similar to that for **2**, two different types of interactions account for the hierarchical growth, of which one arises earlier than the other because of differences in sensitivity for hydrophobicity.

The locking of the disks in a fixed chiral conformation is proposed to be governed by intra- and intermolecular hydrogen bonding with the consecutive molecules mutually twisted in such a way that self-assembled, highly regular chiral columnar stacks are formed. Self-assembly **a** in Figure 11 shows how these molecules can pack into chiral columns. The three wedges on the central core are twisted out of the plane due to steric hindrance, thus providing a scaffold for the packing of the molecules. The second helix (**b**) in Figure 11, in which part of the outer groups are omitted, shows the possibility for the formation of intermolecular hydrogen bonds: due to the rotation of the subsequent molecules and the twist of the wedges (ship screw packing of the molecules),[3] linear intermolecular hydrogen bonding is possible, thus enabling positional locking of the molecules. As has been shown previously,[3,21] intermolecular hydrogen bonding between similar C_3-symmetrical disks is

(20) Chan, H. S.; Bromberg, S.; Dill, K. A. *Philos. Trans. R. Soc. London B* **1995**, *348*, 61.

(21) (a) Brunsveld L.; Schenning, A. P. H. J.; Broeren, M. A. C.; Janssen, H. M.; Vekemans, J. A. J. M.; Meijer, E. W. *Chem. Lett.* **2000**, 292. (b) Yasuda, Y.; Iishu, E.; Inada, H.; Shirota, Y. *Chem. Lett.* **1996**, 575. (c) Yasuda, Y.; Takebe, Y.; Fukumoto, M.; Inada, H.; Shirota, Y. *Adv. Mater.* **1996**, *8*, 740.

highly cooperative and directional and locks the subsequent molecules on top of each other. The creation of a hydrophobic microenvironment by the $\pi-\pi$ stacking of the aromatic cores allows for operation of these secondary interactions in polar media, similar to the way the hydrophobic microenvironment in proteins, which is created by a hydrophobic collapse, allows for the expression of hydrogen bonds.[7] The molecularly dissolved molecules first aggregate into small self-assembled species via hydrophobic interactions. When such self-assemblies are formed, the polar solvent cannot penetrate into the core any longer, resulting in a hydrophobic microenvironment around the inner molecules. With the occurrence of the microenvironment, the native state of the helical structure can be created via the intermolecular hydrogen bonds.

Conclusions

In conclusion, we have demonstrated the creation of well-defined chiral self-assembled structures in protic media invoking a variety of secondary interactions. These interactions occur in a hierarchical fashion, thus giving rise to a stepwise growth of the discotic molecules into chiral columns via intermediates lacking supramolecular chirality. The created hydrophobic microdomain in the achiral aggregates allows the expression of the more sensitive polar interactions. The reversible chiral assemblage and its importance for the hierarchical growth resemble the folding and assembly of proteins and polynucleotides and together with the differences observed for superstructure formation between apolar and polar media gives valuable information for a better understanding of supramolecular architecture formation in protic media.

Experimental Section

General. All starting materials were obtained from commercial suppliers and used as received. All moisture-sensitive reactions were performed under an atmosphere of dry argon. Dry and ethanol-free dichloromethane were obtained by distillation from P_2O_5, dry tetrahydrofuran was obtained by distillation from Na/K/benzophenone, dimethylformamide was dried over BaO, and triethylamine was dried over potassium hydroxide. Analytical thin-layer chromatography was performed on Kieselgel F-254 precoated silica plates. Visualization was accomplished with UV light. Column chromatography was carried out on Merck silica gel 60 (70−230 mesh) or on Merck aluminum oxide 90 (70−230 mesh, activity II−III). Preparative size exclusion chromatography was performed on BIO RAD Bio Beads S-X1 swollen in methylene chloride. ^{1}H NMR and ^{13}C NMR spectra were recorded on a 400 MHz 4-nucleus NMR (Varian Mercury Vx) (400.13 MHz for ^{1}H NMR and 100.62 MHz for ^{13}C NMR). Proton chemical shifts are reported in ppm downfield from tetramethylsilane (TMS) and carbon chemical shifts in ppm downfield of TMS using the resonance of the deuterated solvent as internal standard. Matrix-assisted laser desorption/ionization mass spectra were obtained using indole acrylic acid as the matrix on a PerSeptive Biosystems Voyager-DE PRO spectrometer. IR spectra were measured on a Perkin-Elmer 1600 FT-IR. Optical properties and melting points were determined using a Jeneval polarization microscope equipped with a Linkam THMS 600 heating device with crossed polarizers. DSC spectra were obtained on a Perkin-Elmer Pyris 1 DSC. Ultrasensitive differential scanning microcalorimeter measurements were recorded on a VP-DSC from Heath Scientific. X-ray diffraction patterns were recorded using a multiwire area detector X-1000 coupled with a graphite monochromator. GPC measurements were carried out using a column with PL gel and chloroform as eluent and a flow rate of 1 mL min^{-1}; detection was carried out on a UV detector at a wavelength of 254 nm. GC-MS measurements were performed on a Shimadzu GCMS QP5000. UV−vis spectra were recorded on a Perkin-Elmer Lambda 900 UV/vis/NIR spectrometer. CD spectra were recorded on a Jasco J-600 spectropolarimeter. Fluorescence emission spectra were recorded on a Perkin-Elmer LS50B luminescence spectrometer. The femtosecond fluorescence upconversion transients were measured using the setup (time resolution: $\sim$ 150 fs) described previously.[15] Fluorescence transient measurements with picosecond time resolution were conducted using time-correlated single-photon-counting detection.[18] The syntheses of 2,2′-bipyridine-3,3′-diamine (**5**),[22] (2*S*)-ethyl-2-(tetrahydropyran-2-yloxy)propionate (**10**),[23] (2*S*)-2-(tetrahydropyran-2-yloxy)propan-1-ol (**11**),[23] and compounds **18a**−**c**[24] have been described previously.

***N*,*N*′,*N*″-Tris{3[3′-(3,4,5-tris{(2*S*)-2-(2-{2-[2-(2-methoxyethoxy)ethoxy]ethoxy}ethoxy)propyloxy})benzoylamino]-2,2′-bipyridyl}-benzene-1,3,5-tricarbonamide (2).** To an ice-cooled solution of **4** (1.00 g, 0.92 mmol) and triethylamine (0.14 mL, 1.0 mmol) in dry methylene chloride (10 mL) was added a solution of trimesic chloride (**3**) (79 mg, 0.30 mmol) in dry methylene chloride (5 mL) dropwise at room temperature. The resulting mixture was stirred at room temperature overnight, and the solvents were evaporated in vacuo. The crude product was purified by column chromatography (silica; 5% methanol in methylene chloride) and preparative size exclusion chromatography (methylene chloride) to give **2** as an off-white wax (0.87 g, 0.247 mmol, 82%): T_{cl} = 270 °C; ^{1}H NMR ($CDCl_3$) δ = 15.52 (s, 3H), 14.42 (s, 3H), 9.60 (dd, J = 8.5 and 1.2 Hz, 3H), 9.40 (dd, J = 8.5 and 1.4 Hz, 3H), 9.30 (s, 3H), 9.07 (dd, J = 4.6 and 1.4 Hz, 3H), 8.53 (dd, J = 4.4 and 1.3 Hz, 3H), 7.58 (m, 6H), 7.32 (s, 6H), 4.18−4.15 (m, 9H), 4.05−3.90 (m, 18H), 3.90−3.72 (m, 27H), 3.71−3.60 (m, 99H), 3.59−3.52 (m, 18H), 3.37 (m, 27H), 1.33 (m, 27H); ^{13}C NMR ($CDCl_3$) δ = 165.8, 164.0, 152.6, 142.2, 141.6, 141.5, 140.6, 137.4, 137.3, 136.0, 130.4, 130.0, 129.8, 129.5, 124.6, 124.2, 107.5, 76.3, 75.0, 74.3, 73.1, 71.8, 70.8, 70.7, 70.5 (3×), 70.4 (2×), 68.8, 68.5, 89.9, 17.5; MALDI-TOF [M + Na$^+$] = calcd 3428.7 Da, obsd 3428.1 Da.

3′-{3,4,5-Tris[(2*S*)-2-(2-{2-[2-(2-methoxyethoxy)ethoxy]ethoxy}-ethoxy)propy1oxy]benzoylamino}-2,2′-bipyridine-3-amine (4). To a solution of **8** (2.6 g, 2.8 mmol) and two drops of dry dimethylformamide in dry methylene chloride (10 mL) was added a solution of oxalyl chloride (0.39 g, 3.1 mmol) in methylene chloride (5 mL) dropwise. The mixture was stirred overnight at room temperature in the absence of light, and subsequently the solvent was removed by evaporation in vacuo and the compound (**7**) was dried under vacuum (1 mbar) for 2 h. The product was dissolved in dry methylene chloride (20 mL) and added dropwise via a syringe to an ice-cooled, magnetically stirred solution of 2,2′-bipyridine-3,3′-diamine (**5**) (0.521 g, 2.8 mmol) and triethylamine (0.38 mL, 2.8 mmol) in dry methylene chloride (25 mL). Stirring was continued for another 2 h at 0 °C and subsequently overnight at room temperature. The solution was diluted with methylene chloride, washed with water (2×) and brine (1×), and dried over sodium sulfate, and the solvents were evaporated in vacuo. The crude product was purified by column chromatography (silica; 5% methanol in methylene chloride) and preparative size exclusion chromatography (methylene chloride) to yield the title compound as a yellow oil (2.2 g, 2.03 mmol, 78%). The product was thoroughly dried in vacuo over P_2O_5: ^{1}H NMR ($CDCl_3$) δ = 14.40 (s, 1H), 9.21 (dd, J = 8.5 and 1.7 Hz, 1H), 8.33 (dd, J = 4.6 and 1.5 Hz, 1H), 8.03 (dd, J = 3.9 and 1.8 Hz, 1H), 7.33 (m, 3H), 7.15 (m, 2H), 6.57 (s, 2H), 4.12−4.05 (m, 3H), 3.98−3.53 (m, 54H), 3.38 (s, 3H), 3.37 (s, 6H), 1.32 (m, 9H); ^{13}C NMR ($CDCl_3$) δ = 165.7, 152.4, 145.1, 143.6, 141.2, 140.8, 138.4, 135.9, 134.8, 130.7, 128.5, 125.2, 124.2, 122.7, 106.7, 76.3, 75.0, 74.3, 72.9, 71.8, 70.7, 70.4, 70.3, 68.8, 68.5, 58.9, 17.4.

3,4,5-Tris[(2*S*)-2-(2-{2-[2-(2-methoxyethoxy)ethoxy]ethoxy}ethoxy)-propyloxy]benzoic Acid (8). A solution of **9** (2.80 g, 3.0 mmol) and KOH (85%) (0.53 g, 9.0 mmol) in ethanol (20 mL) and water (20 mL) was heated under reflux overnight. Subsequently, the solution was acidified to pH = 2 with concentrated hydrochloric acid under reflux and then the solution was poured onto an water/ice mixture. The aqueous layer was extracted with methylene chloride (2×). The

(22) Kaczmarek, L.; Nantka-Namirski, P. *Acta Polon. Pharm.* **1979**, *6*, 629.

(23) (a) Perkins, M. V.; Kitching, W.; König, W. A.; Drew, R. A. I. *J. Chem. Soc., Perkin Trans. 1* **1990**, 2501. (b) Cowie, J. M. G.; Hunter, H. W. *Makromol. Chem.* **1990**, *191*, 1393. (c) Chiellini, E.; Galli, G.; Carrozzino, S. *Macromolecules* **1990**, *23*, 2106.

(24) Palmans, A. R. A.; Vekemans, J. A. J. M.; Meijer, E. W. *Recl. Trav. Chim. Pays-Bas* **1995**, *114*, 277.

combined organic layers were washed with brine (pH = 2) and dried over magnesium sulfate, and evaporation of the solvent in vacuo afforded pure **8** as a colorless oil (2.7 g, 2.95 mmol, 98%): ^{1}H NMR ($CDCl_3$) δ = 7.33 (s, 2H), 4.12−4.05 (m, 3H), 3.98−3.88 (m, 9H), 3.86−3.53 (m, 45H), 3.38 (s, 3H), 3.37 (s, 6H), 1.32 (m, 9H); ^{13}C NMR ($CDCl_3$) δ = 168.9, 152.0, 142.3, 124.5, 108.6, 76.0, 74.9, 74.2, 72.5, 71.7, 70.7, 70.6, 70.4, 70.3, 70.2, 68.7, 68.4, 58.8, 17.3.

Methyl 3,4,5-Tris[(2*S*)-2-(2-{2-[2-(2-methoxyethoxy)ethoxy]ethoxy}-ethoxy)propyloxy]benzoate (9). A mixture of **17** (5.60 g, 13.3 mmol), methyl 3,4,5-trihydroxybenzoate (0.73 g, 4.0 mmol), and K_2CO_3 (5.5 g, 40 mmol) in dimethylformamide (40 mL) was stirred overnight at 70 °C. After cooling, the mixture was poured into water (200 mL, pH = 2) and extracted with methylene chloride. The organic layer was washed with water (3×) and brine (1×) and dried over magnesium sulfate, and the solvent was evaporated in vacuo. The crude product was purified by column chromatography (alumina; 1% ethanol in methylene chloride) to yield the pure compound as a viscous colorless oil (2.9 g, 3.1 mmol, 78%): ^{1}H NMR ($CDCl_3$) δ = 7.30 (s, 2H), 4.12−4.05 (m, 3H), 3.98−3.85 (m, 6H), 3.89 (s, 3H), 3.84−3.50 (m, 48H), 3.37 (s, 3H), 3.36 (s, 6H), 1.32 (m, 9H); ^{13}C NMR ($CDCl_3$) δ = 166.6, 152.2, 142.0, 124.9, 108.2, 76.3, 75.0, 74.3, 72.6, 71.9, 70.8, 70.5, 70.4, 68.8, 68.5, 59.0, 52.2, 17.5.

(2*S*)-1-Benzyloxy-2-(tetrahydropyran-2-yl-oxy)propane (12). A solution of *t*-BuOK (78.5 g, 0.70 mol) in *tert*-butyl alcohol (570 g) was added dropwise to **11**. The solution was stirred for 2 h, concentrated, and subsequently diluted with dioxane (400 mL). A catalytic amount of tetrabutylammonium chloride (2 g) was added after which benzyl chloride (88.6 g, 0.70 mol) was added dropwise at room temperature. The mixture was heated at 80 °C overnight. After reaction, water was added, and the mixture was extracted with diethyl ether (3×). The organic layers were combined and back-washed with water and brine, subsequently dried over magnesium sulfate, and concentrated in vacuo, leaving a yellow oil. Distillation (118 °C, 5×10^{-2} mbar) gave the pure title compound as a colorless oil (99.3 g, 0.40 mol, 64%): ^{1}H NMR (400 MHz, $CDCl_3$) δ = 7.40−7.20 (m, 5H), 4.78 (dt, 1H), 4.56 (d, 2H), 4.07−3.90 (m, 2H), 3.62−3.42 (m, 3H), 1.90−1.80 (m, 1H), 1.80−1.68 (m, 1H), 1.65−1.50 (m, 4H), 1.27−1.15 (m, 3H); ^{13}C NMR (100 MHz, $CDCl_3$) δ = 138.5, 138.4, 128.3, 128.2, 127.5, 127.4, 127.4, 98.8, 96.1, 74.3, 74.2, 73.2, 73.1, 71.9, 70.4, 62.7, 62.2, 31.0, 31.0, 25.5, 19.9, 19.5, 18.6, 16.6.

(2*S*)-1-Benzyloxypropan-2-ol (13). To an ice-cooled solution of **12** (98 g, 0.39 mol) in methanol (500 mL) was added *p*-TsOH·H_2O (3 g, 18 mmol). The solution was subsequently stirred at room temperature overnight. $NaHCO_3$ was added to quench the reaction. The methanol was evaporated, and additional coevaporation with methanol was performed to make sure that all dihydropyran (DHP) was also removed. Water/diethyl ether extraction, drying of the collected organic layers with magnesium sulfate, and evaporation of the solvent gave the crude yellow product. Distillation (91 °C, 8×10^{-1} mbar) gave the pure title compound as a colorless oil (56.0 g, 0.34 mol, 86%): ^{1}H NMR (400 MHz, $CDCl_3$) δ = 7.37−7.24 (m, 5H), 4.54 (s, 2H), 4.00−3.95 (m, 1H), 3.46−3.25 (m, 2H), 1.13 (d, 3H); ^{13}C NMR (100 MHz, $CDCl_3$) δ = 137.9, 128.4, 127.7 (2×), 75.8, 73.2, 66.4, 18.6.

2-{2-[2-(2-Methoxyethoxy)ethoxy]ethoxy}ethyl *p*-Tosylate (14). NaOH (9.9 g, 0.25 mol) and 2-{2-[2-(2-methoxyethoxy)ethoxy]ethoxy}-ethanol (36.0 g, 0.173 mol), in a two-phase system of water (50 mL) and THF (400 mL), was cooled via an ice bath with magnetic stirring. *p*-Toluenesulfonyl chloride (36.2 g, 0.190 mol) in tetrahydrofuran (50 mL) was added dropwise to the mixture, while maintaining the temperature below 5 °C. The solution was stirred at 0 °C for another 3 h and then poured into ice−water (100 mL). The mixture was extracted with methylene chloride (3 × 100 mL), and the combined organic layers were washed with water (pH = 1) (2×) and with brine (1×). After drying over magnesium sulfate, the solvent was evaporated in vacuo to yield the pure compound as a colorless oil (60.7 g, 0.167 mol, 97%): ^{1}H NMR (400 MHz, $CDCl_3$) δ = 7.79 (d, 2H), 7.35 (d, 2H), 4.15 (t, 2H), 3.68 (t, 2H), 3.67−3.58 (m, 10H), 3.54 (t, 2H), 3.36 (s, 3H), 2.44 (s, 3H); ^{13}C NMR (100 MHz, $CDCl_3$) δ = 144.6, 132.7, 129.5, 128.0, 71.8, 70.6 (2×), 70.4 (2×), 70.3, 69.1, 68.5, 58.8, 21.4.

(2*S*)-1-Benzyloxy-2-(2-{2-[2-(2-methoxyethoxy)ethoxy]ethoxy}-ethoxy)propane (15). A solution of **13** (19.9 g, 0.120 mol) **14** (50.0 g, 0.138 mol) and KOH (26.6 g, 0.404 mol) in tetrahydrofuran (350 mL) was stirred under reflux for 12 h under an argon atmosphere. Subsequently water (50 mL) was added to hydrolyze the excess of **14** to the corresponding alcohol. Water/diethyl ether extraction, drying of the collected organic layers with magnesium sulfate, and evaporation of the solvent gave the crude yellow product. Kugelrohr distillation (225 °C, 5×10^{-2} mbar) gave the pure title compound as a colorless oil (37.6 g, 0.105 mol, 88%): ^{1}H NMR (400 MHz, $CDCl_3$) δ = 7.35−7.22 (m, 5H), 4.53 (d, 2H), 3.71−3.37 (m, 19H), 3.35 (s, 3H), 1.15 (d, 3H); ^{13}C NMR (100 MHz, $CDCl_3$) δ = 138.3, 128.3, 127.5, 127.4, 75.0, 74.0, 73.2, 71.8, 70.8, 70.5 (3×), 70.4, 68.5, 59.0, 17.2.

(2*S*)-2-(2-{2-[2-(2-Methoxyethoxy)ethoxy]ethoxy}ethoxy)propan-1-ol (16). The benzyl-protected precursor **15** (37.0 g, 0.104 mol) was dissolved in ethanol (96%) (100 mL) and acidified with hydrochloric acid (0.1 mL, 37%). A catalytic amount of Pd/C (10%) was added to the solution, and hydrogenation at 50 psi H_2-overpressure was carried out during 4 h. Filtration, evaporation of the solvents, and Kugelrohr distillation (175 °C, 5×10^{-2} mbar) gave the pure title compound as a colorless oil (26.4 g, 0.099 mol, 95%): ^{1}H NMR (400 MHz, $CDCl_3$) δ = 3.85−3.78 (m, 1H), 3.69−3.43 (m, 18H), 3.36 (s, 3H), 2.99 (bs, 1H) 1.12 (d, 3H); ^{13}C NMR (100 MHz, $CDCl_3$) δ = 76.7, 71.8, 70.7, 70.5 (3×), 70.4, 68.0, 66.2, 58.9, 16.2. $[\alpha]^{20}_D$ (c = 0.88; chloroform) = +13.3°.

(2*S*)-2-(2-{2-[2-(2-Methoxyethoxy)ethoxy]ethoxy}ethoxy)propane-1-*p*-tosylate (17). NaOH (0.92 g, 0.023 mol) and **16** (4.0 g, 0.015 mol), in a two-phase system of water (4 mL) and tetrahydrofuran (4 mL), was cooled via an ice bath with magnetic stirring. *p*-Toluenesulfonyl chloride (3.3 g, 0.017 mol) in tetrahydrofuran (4 mL) was added dropwise to the mixture, while maintaining the temperature below 5 °C. The solution was stirred at 0 °C for another 3 h and then poured into ice−water (25 mL). The mixture was extracted with methylene chloride (3 × 25 mL), and the combined organic layers were washed with water (pH = 1) (2×) and with brine (1×). After drying over magnesium sulfate, the solvent was evaporated in vacuo to yield the pure compound as a colorless oil (5.7 g, 0. 013 mol, 89%): ^{1}H NMR (400 MHz, $CDCl_3$) δ = 7.81 (d, 2H), 7.36 (d, 2H), 4.00−3.88 (m, 2H), 3.70−3.50 (m, 17H), 3.36 (s, 3H), 2.45 (s, 3H), 1.14 (d, 3H); ^{13}C NMR (100 MHz, $CDCl_3$) δ = 144.5, 132.7, 129.6, 127.7, 73.4, 72.5, 71.8, 70.6, 70.5 (2×), 70.4 (3×), 68.8, 58.9, 21.6, 16.7.

Acknowledgment. The National Research School Combination: Catalysis is thanked for funding. We thank Joost van Dongen for MALDI-TOF/MS measurements. Koen Pieterse is kindly acknowledged for creation of Figure 11.

Supporting Information Available: ^{1}H and ^{13}C NMR of compounds **2**, **4**, **7**−**9**, and **15**−**17**. This material is available free of charge via the Internet at http://pubs.acs.org.

JA0005237